



## Paleotsunamis from the central Kuril Islands segment of the Japan-Kuril-Kamchatka subduction zone

Breanyn MacInnes<sup>a,\*</sup>, Ekaterina Kravchunovskaya<sup>†</sup>, Tatiana Pinegina<sup>b</sup>,  
Joanne Bourgeois<sup>c</sup>

<sup>a</sup> Department of Geological Sciences, Central Washington University, 400 E University Way, Ellensburg, WA 98926-7418, USA

<sup>b</sup> Institute of Volcanology and Seismology, Far Eastern Branch, Russian Academy of Sciences, Petropavlovsk-Kamchatskiy, 683006, Russia

<sup>c</sup> Department of Earth and Space Sciences, University of Washington, Seattle, WA 98195, USA

### ARTICLE INFO

#### Article history:

Received 16 July 2015

Available online 27 May 2016

#### Keywords:

Tsunami

Paleotsunami

Kuril Islands

### ABSTRACT

Paleotsunami records from the central Kuril Island segment of the Japan-Kuril-Kamchatka subduction zone indicate that the region has been frequently inundated by tsunamis. As many as 20–22 tsunami deposits are recognized on Matua Island for the past 3300 yr with an average tsunami recurrence interval of ~150 yr, and 34–36 tsunami deposits are evident on Simushir Island for the past 2350 yr with an average recurrence of ~65 yr. These intervals are short, but comparable to other segments of the Japan-Kuril-Kamchatka subduction zone. Results from all survey locations reveal shortening recurrence intervals toward the present, especially for the last 600 yr, indicating a possible preservation bias. On Simushir, tsunamis at least 11 m higher than the modern tsunamis in 2006 and 2007 occurred every ~300 yr on average. On Matua, tsunamis with slightly farther inundation than the 2006 and 2007 tsunamis occurred every ~215 yr while those with at least 100 m farther inland inundation occur every ~750 yr. Our paleotsunami record almost certainly includes tsunamis that are not from great subduction zone earthquakes in the central Kuril segment: we expect the Matua record includes volcanic tsunamis and the Simushir record includes tsunamis from the southern Kuril segment.

© 2016 University of Washington. Published by Elsevier Inc. All rights reserved.

### Introduction

The Japan-Kuril-Kamchatka (JKK) subduction zone, from northern Japan to the central Kamchatka Peninsula (Fig. 1), is one of the most active tectonic regions of the world, producing tsunami-genic earthquakes virtually every decade in instrumental history (NGDC/WDS, 2014). However, because recurrence intervals of great earthquakes are often of longer duration than recorded history, the length of seismic cycles for many segments of subduction zones cannot be estimated with the historical record alone. A case in point is the remote and sparsely populated central Kuril Islands, where paleotsunami deposits are the only means for generating a robust paleoseismic record.

Determining the frequency of tsunamis initiated by subduction zone earthquakes is important to local communities and those farther afield since they can have damaging trans-oceanic effects.

Tsunamis originating along the JKK subduction zone propagate toward the Americas, with historical examples including 1952 southern Kamchatka ( $M_w$  9.0; Okal, 1992) and 2011 Tohoku ( $M_w$  9.0; Ide et al., 2011). From the central Kurils, the 2006 ( $M_w$  8.3) earthquake produced a tsunami with highest trans-Pacific amplitudes in northern California, Hawaii, and Chile, and resulted in \$9.2 million in damage in Crescent City, California (Dengler et al., 2009).

Paleotsunami deposits are key to extending the record of seismicity beyond the scope of human history. For example, deposits from Cascadia and northern Japan indicate average recurrence of tsunamis of ~500 yr (Clague et al., 2000; Nanayama et al., 2003; Witter et al., 2003; Kelsey et al., 2005). Shorter average intervals are revealed by deposits in Chile (80–100 yr; Ely et al., 2014; Dura et al., 2015) and the eastern Aleutians (180–270 yr; Nelson et al., 2015). Deposits can also indicate periods of increased seismicity or of quiescence (Pinegina et al., 2003; Kelsey et al., 2005; Razzhigaeva et al., 2008). Furthermore, the extent (inland and alongshore) of paleotsunami deposits can help determine the magnitude of paleoearthquakes (Nanayama et al., 2003; Nelson et al., 2006; Pinegina, 2014).

\* Corresponding author.

E-mail address: [macinnes@geology.cwu.edu](mailto:macinnes@geology.cwu.edu) (B. MacInnes).

† Deceased.

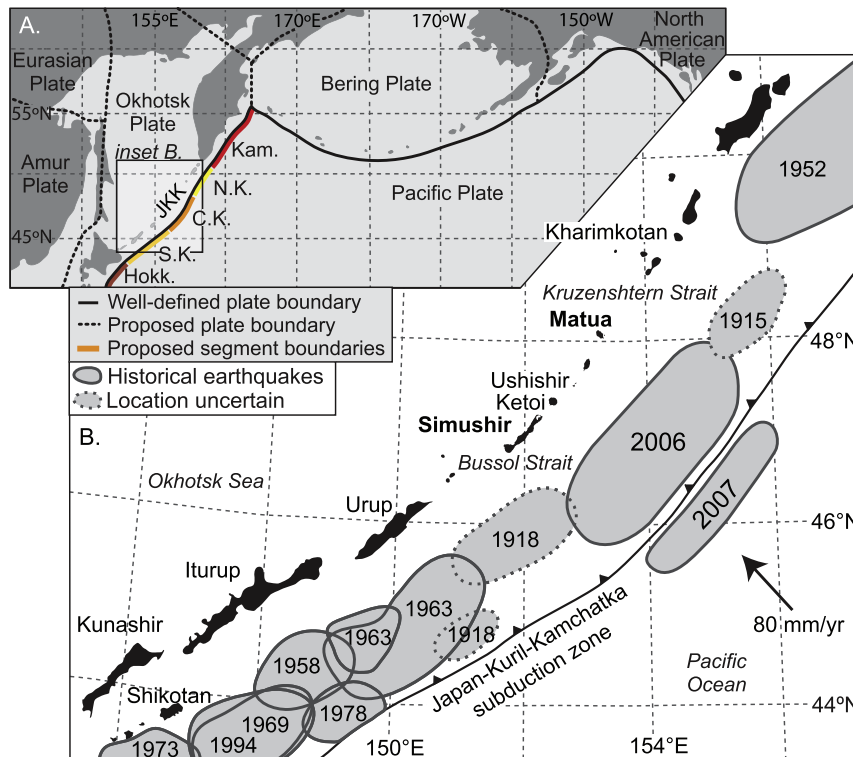


**Figure 1.** (A) Tectonic setting of the Kuril Islands, modified from Mackey et al. (1997) and Apel et al. (2006). Labels are as follows: JKK = Japan-Kuril-Kamchatka subduction zone, Kam. = Kamchatka segment, N.K. = northern Kuril segment, C.K. = central Kuril segment, S.K. = southern Kuril segment, and Hokk. = part of Hokkaido segment. The southernmost (Tohoku) segment of the JKK is not shown. (B) Historical earthquakes that produced tsunamis with recorded heights of at least 0.5 m in the southern, central, and northern Kuril segments of JKK (with the exception of 1915, after Fedotov et al. (1982) and the NGDC/WDS database. Earthquake locations prior to 1915 are too uncertain to map. The 2007 earthquake was an outer-rise event in the Pacific Plate. Labeled place names are referred to in the text.

The history of paleotsunamis in the central Kurils was unknown prior to investigations during the Kuril Biocomplexity Project's field campaigns of 2006–2008 (c.f. Fitzhugh, 2012; Fitzhugh et al., 2016). Besides the challenge of their remoteness, these rugged islands have few coastal plains capable of preserving extensive paleotsunami records. The best Pacific-facing sites in the central Kurils, Yuzhnaya Bay and Ainu Bay on Matua Island and Dushnaya Bay on Simushir Island (Figs. 1 and 2), were used in our study to determine the record and recurrence of tsunamis that affected the region. Observations of runup, inundation, erosion, and deposition by recent tsunamis help calibrate the paleotsunami

record. Runup is defined as the tsunami elevation at maximum tsunami inundation, which is the horizontal distance inland that a tsunami reaches. Abundant tephra layers aid in correlation, dating, and paleogeographic reconstruction.

**Background**

*Setting*

The central Kuril Island segment of the JKK subduction zone is defined as between the Bussol and Kruzenshtern straits (Fig. 1), a

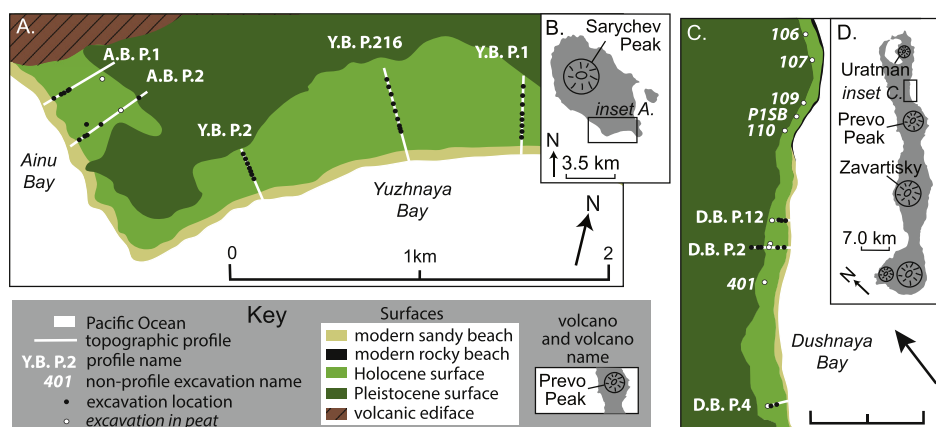


**Figure 2.** Environments and landforms of (A) Ainu and Yuzhnaya bays on (B) Matua Island and (C) Dushnaya Bay on (D) Simushir Island. Outlines of (A) and (C) are noted on (B) and (D). Locations of topographic profiles and excavations are noted. For names of excavations along profiles, see excavation stratigraphy illustrated in Supplementary Figures 5–12. Only volcanoes referred to in the text are named.

geographically complicated region with generally smaller islands than elsewhere in the Kuril volcanic arc. Here, the Pacific plate, dated to 100–120 Ma, subducts under the Okhotsk plate at a rate of ~81 mm/yr (Bird, 2003).

Matua Island (~50 km<sup>2</sup>) lies at the northern end of the central Kurils, slightly west of other central islands, while Simushir Island (~340 km<sup>2</sup>) lies at the southern end (Fig. 1). The Japanese heavily occupied Matua during World War II (WWII), but Simushir was only sparsely occupied. Prior to WWII, Simushir had few historical settlements, Matua apparently none. In the central Kurils, historical records associated with explorers, fur traders and fishermen are spotty, but extend to the 1700s (Golder, 1914; Ogryzko, 1953; Krasheninnikov, 1972). Evidence of human occupation by maritime hunter-gatherers is present on both islands, dating back at least 2200 yr (Fitzhugh, 2012; MacInnes et al., 2014). Three main study areas were examined, which include:

#### *Yuzhnaya Bay, Matua Island*

This site is a prograding, vegetated beach-ridge plain at 5–9 m elevation, backed by a steep slope leading to a tilted, 40–80-m-high terrace (Fig. 2A). There are no streams in the bay. Prominent beach ridges in Yuzhnaya Bay can be correlated along the length of the embayment; smaller ridges appear and disappear. The modern beach is sandy and open to the Pacific, with a few exposed basalt outcrops offshore.

#### *Ainu Bay, Matua Island*

A large section of the coastal plain is a *Carex* marsh surface at 11–12 m elevation backed by a slope leading to a 20-m terrace, and fronted by a narrow, vegetated beach-ridge plain (Fig. 2A). The marsh is fed by springs and drains through a small stream. The stream fed a small lake that was breached by the most recent tsunami (discussed below) and the seaward-most beach ridge eroded away (MacInnes et al., 2009a,b). The modern beach is sandy and open to the southwest, with bedrock outcrops offshore at the north and south ends.

#### *Dushnaya Bay, Simushir Island*

This long embayment stretches from Prevo to Uratman volcanoes (Fig. 2D). The surveyed section of Dushnaya Bay consists of a prograding, vegetated beach-ridge plain at 4–9 m elevation, backed by a steep slope up to a 20–40-m-high Pleistocene terrace (Fig. 2C). The modern beach is primarily sandy, with a few exposed basalt outcrops offshore; the shoreline is rockier toward the north.

#### *Historical tsunamis*

The most recent great earthquakes in the central Kuril region were the subduction-zone and outer-rise doublet of 15 November 2006 ( $M_w$  8.3) and 13 January 2007 ( $M_w$  8.1) (Fig. 1) (Ammon et al., 2008); both produced tsunamis. Post-tsunami survey runup measurements averaged 6.5 m in Yuzhnaya Bay and 17 m in Ainu Bay. Tsunami runup was 15–20 m at the north and south ends of Dushnaya Bay, respectively, but only 5–8 m on the central coastal plain (MacInnes et al., 2009a) at our study site. All three localities were covered with sandy tsunami deposits up to 90% of the water inundation distance determined by floating debris (MacInnes et al., 2009b). Which tsunami (2006 or 2007) was the primary generator of the surveyed runup and deposits is unknown, though modeling suggests that on Matua Island in particular, 2007 may have been larger than 2006 (Rabinovich et al., 2008; MacInnes, 2010). The combined event is referred to as “2006/2007” in this paper because these two tsunamis’ deposits cannot be confidently differentiated in the surveyed area.

Though many large tsunamigenic earthquakes have occurred historically along the JKK subduction zone (Fig. 1), few, if any, ruptured in the central Kuril segment. Prior to 2006, the central Kurils were considered a seismic gap (Fedotov, 1965; Laverov et al., 2006) or a segment of low seismic potential (Song and Simons, 2003). A large earthquake in 1780 produced a tsunami with reports on Urup, Simushir and Ketoi islands (Lensen, 1959; Soloviev and Ferchev, 1961). Laverov et al. (2006) assigned the earthquake to the central Kuril segment, but it may have been located in the southern Kurils because the tsunami was largest on Urup (Lensen, 1959); its northern extent is uncertain (Lay et al., 2009). An earthquake rupture with its proposed epicenter in the northern Kurils in 1915, estimated  $M_w$  7.7–8.1, may have extended from the north across the Kruzenshtern Strait into the central Kurils (Geller and Kanamori, 1977; Pacheco and Sykes, 1992), although no reports exist of an associated tsunami. Two 1918 earthquakes occurred just south of the Bussol Strait and potentially were a subduction-zone/outer-rise doublet like 2006 and 2007 earthquakes (Lay et al., 2009); the first may have ruptured across the strait into the central Kuril segment (Fedotov, 1965), but this is also uncertain (Beck and Ruff, 1987). Beck and Ruff (1987) considered the northern limit of the 1963 southern Kuril earthquake rupture to be the Bussol Strait, although Hatori (1971) extended the limit farther north, into the central Kurils.

In addition to earthquake-generated tsunamis, volcanogenic tsunamis are known or postulated from locations throughout the Kuril Islands. The most notable observed event was the large 1933 tsunami from the sector collapse of Kharimkotan volcano (Severgin), which had runup up to 20 m (Miyatake, 1934).

#### *Earthquake frequencies and paleotsunamis along the JKK subduction zone – prior work*

Previous studies have estimated recurrence intervals of large earthquakes and tsunamis along most of the JKK subduction zone. The duration of the seismic cycle of earthquakes ( $M_w > 7.75$ ) along the entire zone was first estimated from historical data as  $140 \pm 60$  yr (Fedotov, 1968). More recent studies have focused on specific segments, as summarized below; the central Kurils are omitted here and covered later in the paper.

The northern segments comprising Kamchatka and the northern Kuril Islands are capable of producing  $M_w$  9.0 earthquakes, exemplified by the 1737 and 1952 Kamchatka earthquakes (Fig. 1). Evidence for numerous tsunamis in the last 7000 yr is preserved along the Kamchatka coast—an average recurrence (in southern Kamchatka) of 70–100 yr, but maybe as short as 37 yr (Pinegina, 2014). In the northern Kurils, one tsunami deposit is preserved on average every 90 yr for the last 2500 yr (Pinegina, 2014).

The most active section of the JKK subduction zone historically is the southern Kuril Islands and Hokkaido sections (Fig. 1), with nine  $M_w$  7.5–8.5 earthquakes since 1918 (NGDC/WDS, 2014). Paleotsunami studies on Shikotan Island, at the very southern end of the Kuril Island chain, indicate that one tsunami per 250 yr is common with a minimum recurrence interval of 75 yr (Razhigaeva et al., 2008). Larger earthquakes estimated as  $M_w$  9.0 occur only every ~500 yr on Iturup Island (Iliev et al., 2005; Ganzey et al., 2011). Sawai et al. (2009) notes that on Hokkaido, “outsized tsunamis” average every 400 yr, but range between 100 and 800 over a 6000-yr record.

#### *Volcanic activity*

In our study, mappable tephra layers are key to establishing a chronological framework. As with earthquakes and tsunamis, the historical record of eruptions (Supplementary Table 1) is short and

potentially spotty. The longer-term geologic record includes distinct marker tephra (tephra found on more than one island) from within and outside the central Kurils (Nakagawa et al., 2008).

Sarychev Peak, the current volcanic edifice on Matua Island, is one of the most active volcanoes in the Kurils, with 16 explosive or effusive eruptions recorded since the mid-1700s (Supplementary Table 1; NGDC/WDS, 2014). Ash columns are common, and pyroclastic flows reached the sea in 1930, 1946 and 2009.

On Simushir, three volcanoes lie within 20 km of Dushnaya Bay—Prevo Peak and Zavaritsky volcanoes to the south and Uratman to the north (Fig. 2D). The recent volcanic history for these volcanoes is less well known than for Sarychev Peak. Historically, both Prevo Peak and Zavaritsky have been active, but with only a few observed eruptions (Supplementary Table 1; NGDC/WDS, 2014). Two additional active volcanoes lie at the southern end of Simushir.

Three marker (regional) tephra with known geochemistry are present in the late Holocene coastal stratigraphy of the central Kurils (Tables 1 and 2; Supplemental Figs. 1 and 2; Nakagawa et al., 2008); all three are present on Matua, but only one (CKr) on Simushir. The youngest (Us-Kr) was produced by a caldera-forming eruption of Ushishir volcano, between Matua and Simushir (Fig. 1). Both Simushir and Matua received tephra CKr from a larger caldera-forming eruption of Medvezhya volcano on Iturup Island in the southern Kurils. The third marker tephra (Sar-1) is from an eruption on Matua.

## Tephra methods and results

### Tephra stratigraphy and age control methods

Throughout the Kuril Islands (2006–2010 and prior), tephra were identified in the field as layers of clean sediment within the soil of an excavation, generally with a uniform mineralogy, and typically well sorted. Stratigraphy is most clear in peat excavations, where relatively fast accumulation rates separate and preserve tephra as distinct layers. Tephra in the central Kurils are typically either cinders (2- to 10-mm sized grains) or silt to very fine sand, or both, commonly sublayered.

Tephra were correlated using physical characteristics (primarily grain size, mineral composition, color, thickness, sublayering), stratigraphic position in an excavation, and in select cases, geochemistry (microprobe analysis of glass components) (Supplementary Figs. 1–4). In cases where multiple tephra originated from eruptions closely

spaced in time (such as tephra C7 and SC8 in Table 1), individual tephra could be identified in excavations into the beach ridge active at the time of deposition. Accumulation of sand in the active ridge occurs quickly and can separate similar-aged tephra that would otherwise appear as one layer (e.g. Fig. 3).

We estimated the age of each tephra using a combination of radiocarbon dating and peat accumulation rates between tephra. Radiocarbon ages for tephra layers (Table 2) are primarily from sub-sampled peat or from charcoal. Radiocarbon ages were calibrated and combined (when more than one age existed per tephra) with OxCal 4.2 (Bronk Ramsey, 2009). Ages for tephra without associated radiocarbon samples were estimated by calculating peat accumulation rates between dated tephra (see Supplementary Tables 2–5).

### Tephra stratigraphy and age control results

The central Kuril tephra provided easy divisions of the stratigraphic record into time increments for study of tsunami recurrence. Ten tephra layers with dated radiocarbon samples of peat and charcoal anchored tephrochronological age control of Matua and Simushir stratigraphy (Tables 1 and 2). We used peat accumulation rates to project ages for the C4, C7, S11, GT, and FC tephra (Supplementary Tables 2–5). The oldest tephra layers dated include 1395–1195 BC in Ainu Bay (tephra S17), AD 410–590 in Yuzhnaya Bay (tephra S11) and 386–311 BC in Dushnaya Bay (tephra CKr).

Dushnaya Bay stratigraphy contained five distinct tephra, of which one was the marker tephra CKr; on Matua, eighteen tephra layers, not counting the 2009 tephra, were identified in Yuzhnaya and Ainu bay excavations (Table 2). In addition to the aforementioned marker tephra, the 15 others are all interpreted to have come from eruptions of Sarychev Peak or its predecessors on Matua (Nakagawa et al., 2008), of which the most prominent are associated with caldera-forming eruptions (SC8 and Sar-1; Laverov et al., 2005). Tephra type sections and more complete descriptions of all tephra are presented in Supplementary Figures 1 and 2.

## Tsunami deposits methods and results

### Profile and excavation methodology

We measured a total of eight topographic profiles with accompanying excavations (Fig. 3, Supplementary Figs. 5–12) at the three

**Table 1**  
Sample locations and analysis of radiocarbon dates used to estimate ages of tephra on Matua and northern Simushir islands.

| Island   | Tephra abbreviation | Excavation                         | Relationship to tephra | Material | Lab ID      | Date ( <sup>14</sup> C) |
|----------|---------------------|------------------------------------|------------------------|----------|-------------|-------------------------|
| Matua    | C4                  | 106                                | 0–1 cm below           | Peat     | Beta-284679 | 170 ± 40                |
| Matua    | SC8                 | AB-1 TP 3                          | 0–5 cm below           | Charcoal | OS-58969    | 610 ± 25                |
| Matua    | SC8                 | 116                                | 3–5 cm below           | Charcoal | Beta-284682 | 620 ± 40                |
| Matua    | S12                 | 13107 <sup>a</sup>                 | 0–1 cm above           | Peat     | LU-5929     | 1750 ± 50               |
| Matua    | UsKr                | 166                                | 0–1 cm above           | Charcoal | OS-67626    | 1970 ± 40               |
| Rasshua  | UsKr                | 1B                                 | 0–2 cm above           | Charcoal | OS-67131    | 1990 ± 30               |
| Ushishir | UsKr                | 07-US-18 <sup>b</sup>              | 0–1 cm below           | Charcoal | IAAA-72953  | 1910 ± 40               |
| Matua    | CKr                 | Fitzhugh et al., 2002              | 0–1 cm above           | Charcoal | AA-42209    | 2178 ± 42               |
| Matua    | CKr                 | Fitzhugh et al., 2002              | 2–4 cm below           | Charcoal | AA-42205    | 2290 ± 43               |
| Matua    | Sar-1               | 07MT4 <sup>b</sup>                 | 1–2 cm below           | charcoal | IAAA-72956  | 2420 ± 30               |
| Matua    | Sar-1               | Fitzhugh et al., 2002 <sup>b</sup> | 0–2 cm below           | Charcoal | AA-40943    | 2345 ± 37               |
| Matua    | S17                 | 07MT5 <sup>b</sup>                 | 0–3 cm below           | Peat     | IAAA-72958  | 3030 ± 30               |
| Simushir | P                   | 1607 <sup>a</sup>                  | 8 cm above in peat     | Peat     | LY-5905     | 80 ± 50                 |
| Simushir | P                   | 1607 <sup>a</sup>                  | directly below in peat | Peat     | LY-5906     | 40 ± 90                 |
| Simushir | CC                  | 1607 <sup>a</sup>                  | 2–3 cm above in peat   | Peat     | LY-5907     | 430 ± 50                |
| Simushir | CC                  | Stream Outcrop                     | 25 cm below in sand    | Charcoal | OS-59191    | 515 ± 35                |
| Simushir | CKr                 | Fitzhugh et al., 2002              | 0–1 cm above           | Charcoal | AA-42209    | 2178 ± 42               |
| Simushir | CKr                 | Fitzhugh et al., 2002              | 2–4 cm below           | Charcoal | AA-42205    | 2290 ± 43               |

<sup>a</sup> Sample collected by N. Razzhigaeva.

<sup>b</sup> Sample collected by M. Nakagawa or Y. Ishizuka.

**Table 2**  
Tephra age estimates from radiocarbon dating (Table 1), peat growth rates, and the historical record on Matua and northern Simushir islands in stratigraphic order. <sup>14</sup>C ages are calibrated and combined (when multiple ages have been obtained) with OxCal 4.2.

| Tephra abbreviation | Age estimation from peat growth <sup>a</sup> | Age estimation from historical record | <sup>14</sup> C calibrated age  |
|---------------------|--|---------------------------------------|---|
| Matua Island        |  |                                       |   |
| 2009                | –  | AD 2009                               | –   |
| C1a                 | –  | AD 1960 or 1946 <sup>b</sup>          | –   |
| C1b                 | –  | AD 1946 or 1930 <sup>b</sup>          | –   |
| C2                  | –  | –                                     | –   |
| C3                  | –  | –                                     | –   |
| C4                  | –  | –                                     | AD 1655–1707 (18%); AD 1718–1826 (46%); AD 1832–1886 (13%); 1912 AD-present (18%) |
| SC5                 | –  | –                                     | –   |
| S6                  | –  | –                                     | –   |
| C7                  | AD 1390–1480                                 | –                                     | –   |
| SC8                 | –  | –                                     | AD 1296–1400 (95%)  |
| S9                  | AD 1240–1350                                 | –                                     | –   |
| SC10                | AD 615–770                                   | –                                     | –   |
| S11                 | AD 410–590                                   | –                                     | –   |
| S12                 | –  | –                                     | AD 244–394 (95%)  |
| UsKr                | –  | –                                     | 4 BC–AD 75 (93%)  |
| CKr                 | –  | –                                     | 386–311 BC (95%)  |
| Sar-1               | –  | –                                     | 490–400 BC (95%)  |
| C16                 | 780 to 690 BC                                | –                                     | –   |
| S17                 | –  | –                                     | 1395–1195 BC (95%)  |
| n. Simushir Island  |  |                                       |   |
| P                   | –  | –                                     | AD 1681–1738 (26%); AD 1803–1937 (69%)  |
| CC                  | –  | –                                     | AD 1408–1448 (95%)  |
| GT                  | AD 1020–1100                                 | –                                     | –   |
| FC                  | AD 390–550                                   | –                                     | –   |
| CKr                 | –  | –                                     | 386–311 BC (95%)  |

<sup>a</sup> Age estimations of undated tephra based on assuming steady accumulation rates between bracketing <sup>14</sup>C-dated tephra in peat excavations. For calculations see Supplementary Tables 3–6.

<sup>b</sup> Large known historical eruptions; see Supplementary Table 1.

field sites, with additional off-profile excavations in Dushnaya Bay (Fig. 2C) during field seasons in 2006, 2007, 2008 and 2010. Topographic profiles were made with a tripod, level and rod, with individual measurement error of 0.3 cm vertically and 30 cm horizontally; this uncertainty does not accumulate except when the level is moved (generally 2–4 times per profile) so cumulative vertical error is <30 cm and horizontal error not more than a few meters. Sea level datum for each profile was recorded as the swash zone at time of measurement. The tidal range is <2 m (1.7 m for Matua; Shevchenko and Ivelskaya, 2015). We did not apply tide corrections because local tide predictions for hundreds of kilometers have not been calibrated recently. Tide tables suggest a maximum of 50 cm difference between profiles from the time of measurement, comparable to the expected uncertainty associated with measuring swash.

Most excavations were made in topographic lows between beach ridges (Figs. 2 and 3; Supplementary Figs. 5–11). In each excavation, the sediment and stratigraphy were described; where present, charcoal and peat were sampled for radiocarbon dating, and some tephra sampled for geochemical analysis. Most excavations used in the paleotsunami-deposit counts are at elevations >5 m above local sea level (elevations in Supplementary Figs. 5–12).

#### Paleotsunami deposits and deposit counts

Paleotsunami deposits were identified as layers of clean sand of mixed mineralogy within the soil of an excavation (as in Bourgeois et al., 2006). Tsunami deposits are extensive and generally continuous sand sheets, but deposits in sandier soil can be difficult to distinguish. Sand layers that were not clearly distinct from surrounding stratigraphy were identified as “possible tsunami” rather than “tsunami” by field researchers (Fig. 3). We estimated the minimum inundation (farthest inland extent of the tsunami) and

runup (elevation of the inundation point) for past events assuming sand layers end between the last excavation with the deposit present and the first excavation without the deposit (as in MacInnes et al., 2010).

We calculated the total number of tsunamis to inundate each locality by first counting the number of tsunami deposits between stratigraphically adjacent tephra for each excavation, then finding the maximum number of deposits between each tephra pair for the entire site. We employed three methods for counting. The first method simply entails counting the number of layers; we included two values, including or excluding layers identified as “possible tsunami”. All methods assume that if a tsunami deposit was present in any excavation, the tsunami inundated at least that far inland, even if correlative deposits were not identified closer to the shoreline, where tsunami deposits are more difficult to distinguish in young, sandy soils influenced by storm waves and wind. Even the 2006/2007 tsunami deposit could not be distinguished on the most proximal beach ridges in the summer 2007 field season because weak underlying soil development did not delimit a lower boundary to the deposit.

The second method of counting, hereafter referred to as the “stingy count”, is an attempt to make observations in peat and non-peat excavations comparable by only counting a tsunami deposit in peat where the thickness exceeded 0.5 cm. The 0.5-cm cut-off is a product of field descriptions; deposits thinner than 0.3 cm were generally not noted in non-peat excavations, and deposits thicker than 0.3 cm were usually rounded to the nearest 0.5 cm. In contrast, in peat excavations sand layers only grains thick were identified.

The third method, referred to as the “profiles-only count”, included only excavations on measured topographic profiles. This method helps to make the records between Matua and Simushir more comparable because Matua locations did not include off-profile excavations.

After making tsunami-deposit counts, we calculated paleotsunami recurrence intervals by dividing the age difference of

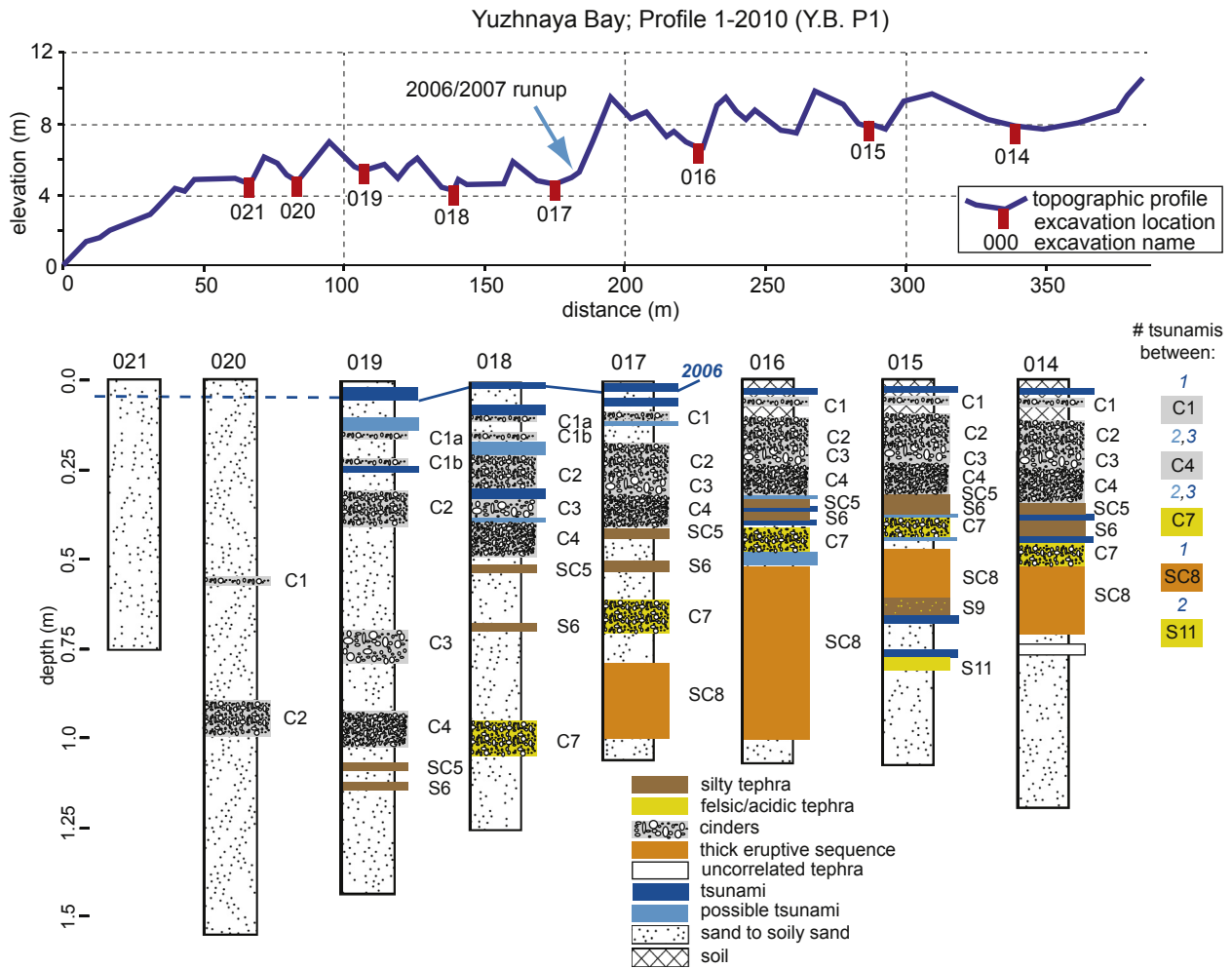


**Figure 3.** Example topography and stratigraphy from Yuzhnaya Bay profile 1–2010. Topographic profile drawing includes the tsunami runup and inundation from either the 2006 or 2007 tsunami. Exact positions of excavation locations are marked. For ages and descriptions of tephra, refer to Table 1 and Supplementary Figures 1–2. The total tsunami statistics for this profile, with the minimum and maximum number of deposits on the profile between given tephra, are shown at the far right. The 2006/2007 tsunami deposit is not counted in these statistics. For all topographic profiles and detailed stratigraphy of all excavations used in this study, refer to Supplementary Figures 5–12.

bracketing tephra by the number of tsunami deposits. Error terms in recurrence intervals include the minimum and maximum for each tephra's age and the presence or absence of “possible” tsunami deposits identified in the field. We also used every possible combination of dated tephra pairs to observe changes in frequency and to see if any particular time interval biased results (Fig. 4).

*Paleotsunami frequency results*

Paleotsunami deposits have similar characteristics to the 2006/2007 deposit. Most paleotsunami deposits were defined by soil horizons above and below the clean (“tsunami”) sand, although it was not unusual for one side of the deposit to be a tephra rather than a soil. In a few instances both sides were defined by tephra. Deposits were typically 1–2 cm thick, rarely exceeding 4 cm, and composed of coarse-very coarse sand (300–400 μm diameter). The sands were well sorted, as are the modern beach sediment samples. Some deposits contained larger grains of rounded, low-density pumice and scoria. No structures or grading were measurable within the deposits, and while the paleotsunami deposits generally thinned landward, average grain size remained constant. We attribute the lack of structure or fining inland as due to a well-

sorted sediment source rather than due to characteristics of the tsunami flow.

We identified up to 20–22 tsunami deposits younger than 3300 yr (above tephra S17) in Ainu Bay (Fig. 4; Supplementary Figs. 5–6 and 10 and 11) in the last 1500 yr (above tephra S11) in Yuzhnaya Bay (Fig. 4; Supplementary Figs. 7–9), an average recurrence interval of 160 ± 15 and 140 ± 20 yr, respectively (Table 3). However, when the record is divided into discrete time intervals, the frequency can be much higher or lower (Fig. 4A and B). One time interval of 500 yr (UsKr to Sar-1, ~AD 50–~450 BC) recorded no tsunami deposits. We find a recurrence interval averaging one tsunami deposit every 55–75 yr since ~AD 1400 in both Ainu and Yuzhnaya bays. The frequency of deposits is significantly less in Ainu Bay before AD 1400, with one sand layer an average of every 250 ± 35 yr (Table 3). The older record in Yuzhnaya Bay is poorly preserved (Fig. 3; Supplementary Figs. 7–9).

Although only separated by a narrow headland, Ainu Bay's tsunami deposits are distinctly more extensive than those in Yuzhnaya Bay. Every tsunami deposit in Ainu Bay is present above 10 m elevation while in Yuzhnaya Bay only half of the deposits can be found above 7.5 m elevation, suggesting tsunamis are predominantly higher in Ainu Bay. Only three event beds extend beyond 300 m inland in Yuzhnaya Bay while as many of two thirds of them

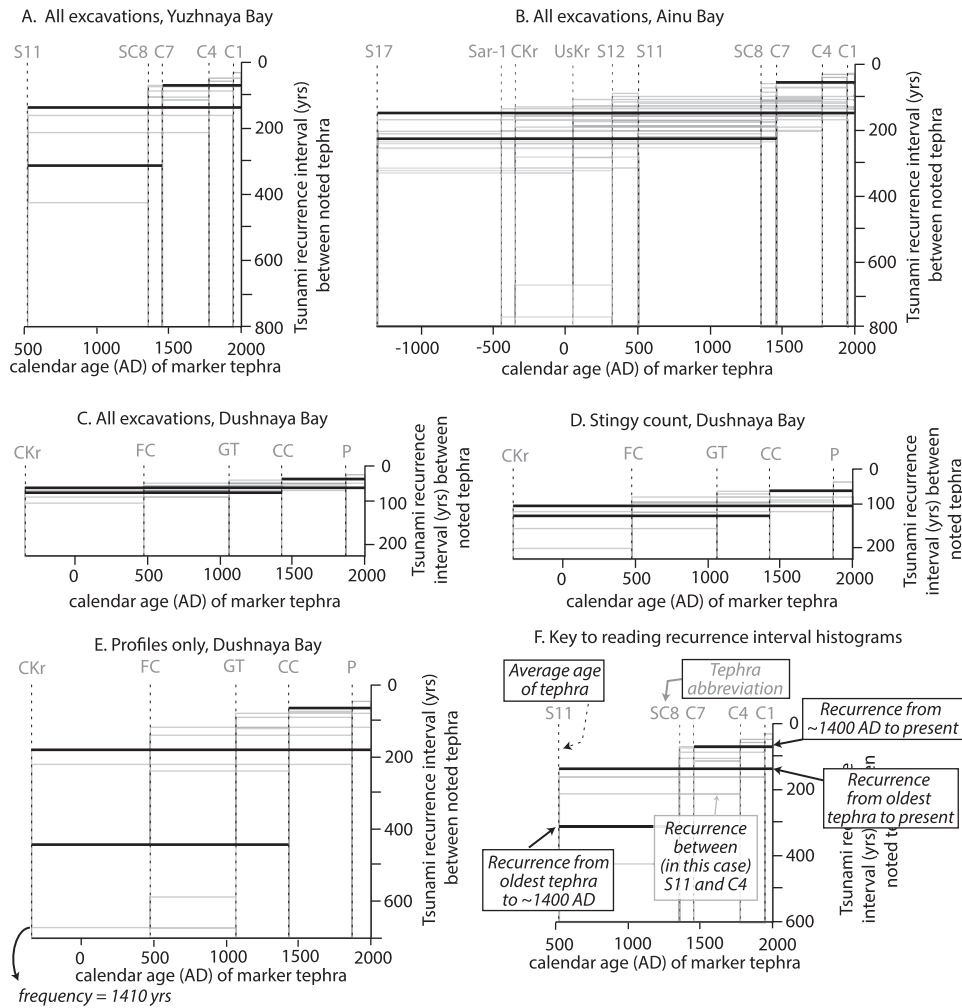


**Figure 4.** Histograms of tsunami recurrence calculations for Yuzhnaya (A), Ainu (B), and Dushnaya (C, D, and E) bays. (F) Illustrates how to read the histograms. Recurrence calculations are based on the maximum number of tsunami deposits at a given site between every possible pair of volcanic tephra; the time interval between the tephra is divided by the number of tsunami deposits. Horizontal black lines represent the recurrence intervals reported in Table 2. Dushnaya Bay graphs show all the excavations (C), only tsunami deposits greater than 0.5 cm thick (D), and only excavations from topographic profiles (E).

**Table 3**  
Overview of tsunami recurrence frequency (years between tsunami deposits) for sites on Matua and Simushir islands; range includes the minimum and maximum number of tsunami deposits and the age range of dated tephra (see Table 2 for dates).

| Tsunami recurrence interval                                     | Matua Island          |          | Dushnaya Bay, Simushir Island |              |                    |
|---|-----------------------|----------|-------------------------------|--------------|--------------------|
|   | Yuzhnaya Bay          | Ainu Bay | All excavations               | Stingy count | Profile-only count |
| Present to oldest tephra  | 145 ± 15              | 160 ± 15 | 65 ± 5                        | 105 ± 5      | 205 ± 30           |
| Present to AD 1400–1450 <sup>a</sup>                            | 75 ± 10               | 55 ± 5   | 45 ± 5                        | 70 ± 5       | 65 ± 5             |
| AD 1400–1450 <sup>a</sup> to oldest tephra                      | 310 ± 45              | 250 ± 35 | 75 ± 5                        | 120 ± 10     | 270 ± 60           |
| Largest tsunamis <sup>b</sup> based on shoreline reconstruction | 215 ± 10 and 750 ± 50 | n/a      | 310 ± 15                      | –            | –                  |

<sup>a</sup> Defined by C7 tephra on Matua and CC tephra on Simushir.

<sup>b</sup> See text for definition of “largest” in the section Comparison of central Kuril sites to other segments of the JKK subduction zone.

exceed 300 m in Ainu Bay, suggesting tsunamis regularly penetrate farther inland in Ainu Bay than Yuzhnaya Bay (Supplementary Tables 6–7).

We identified up to 34–36 tsunami deposits younger than ~2350 yr (above the CKr tephra) in excavations in Dushnaya Bay in Northern Simushir (Fig. 4C, Supplementary Figs. 10–12; Supplementary Table 8). Excluding 2006/2007, 12–13 deposits are younger than ~AD 1400 (above tephra CC), including a sand layer in the middle of tephra P. When we exclude all sand layers thinner

than 0.5 cm in peat excavations, the total number of deposits is 22–23 with 8–9 deposits above tephra CC. The profiles-only count (removes 6 of 20 excavations, including most peat) records 10–13 deposits total, 9 above the CC tephra.

The maximum count of tsunami deposits indicates a frequency of one tsunami every 65 ± 5 yr overall in Dushnaya Bay (Table 3). In all counting methods, the shortest intervals of tsunamis are within the most recent 600 yr (Fig. 4C–E). With all the data used, the frequency between events roughly doubles above the CC tephra. As

the counting methods become more exclusive, the older part of the record is lost, making the difference between recurrence intervals from before ~AD 1400 and those after ~AD 1400 more extreme (Table 3).

Dushnaya Bay excavations were located on two primary surfaces, the lower of which is 4–10 m high (average 6.6 m), extending from the shoreline to a steep slope ~150 m inland. Excavations on the surface above the slope were 17.5–21.5 m high and 200–335 m inland. Four tsunamis reached the higher surface since ~AD 450 (FC tephra), resulting in an average recurrence interval of the largest events of  $310 \pm 15$  yr (Table 3).

**Paleotsunami reconstructions methods and results**

*Methodology for reconstructing paleoshorelines*

Ideally, a reconstruction of the prehistoric coast and hence of paleotsunami size (runup and inundation as approximated by deposit extent) will include an estimate of horizontal shifts of shoreline location for paleo-inundation and an approximation of change in relative sea level for paleo-runup. Previous methods of paleoshoreline reconstructions of beach ridge plains for paleotsunami analysis include direct radiocarbon dating of beach ridge formation (c.f. Sugawara et al., 2010; Tanigawa et al., 2014), or the use of tephra stratigraphy (c.f. Pinegina et al., 2013). All methods make an assumption that no widespread erosion has occurred. Dushnaya and Yuzhnaya profiles both indicate net progradation during the time interval examined (Fig. 5, Supplementary Figs. 13–14). Ainu Bay appears to have had periods of significant erosion in the last few thousand years based on its sedimentology (Supplementary Fig. 15), and therefore it

was not considered for paleoshoreline reconstruction. In general, our paleo-inundation estimates are minima because even though the beach-ridge plains are net progradational, short-lived periods of erosion can remove some of the accumulated coastal width.

The tephra stratigraphy of the prograding beach-ridge plain was used for reconstructing horizontal changes in shoreline position using the methods of Pinegina et al., 2013 (Fig. 5). A tephra deposit is typically preserved in stratigraphy inland from the first dense vegetation (point *dv*) next to the beach. Therefore, the seaward extent of a tephra in the stratigraphy (*dv1*) indicates the *dv* position at the time of eruption (Fig. 5). The *dv1* position is identified as being between the farthest landward excavation without the given tephra and the farthest seaward excavation that includes the tephra. Assuming today's beach width (*bw*) is representative of the past, we estimate the shoreline position at time tephra X to be between the seaward-most excavation with tephra X plus *bw* and the landward-most excavation without tephra X plus *bw* (Fig. 5).

Many profiles show evidence of net positive change in elevation relative to sea level; that is, the shoreward, older parts of profiles are higher than the seaward parts, but reconstructing vertical shoreline changes on volcanic-arc islands is particularly challenging. Such changes in surface elevation can be caused, for example, by volcanic inflation and deflation, by seismic-cycle vertical changes or net tectonic uplift or subsidence, by vertical accumulation via volcanic flows and airfalls, and by changes in regional (eustatic) sea level. The older surfaces in our study are higher than the active beach ridges today, suggesting net uplift of the coast. In this case, our paleo-runup estimates could be too high. Also, all sites are within 5–7 km of active volcanic edifices, so episodes of volcanic inflation and/or deflation likely occurred.

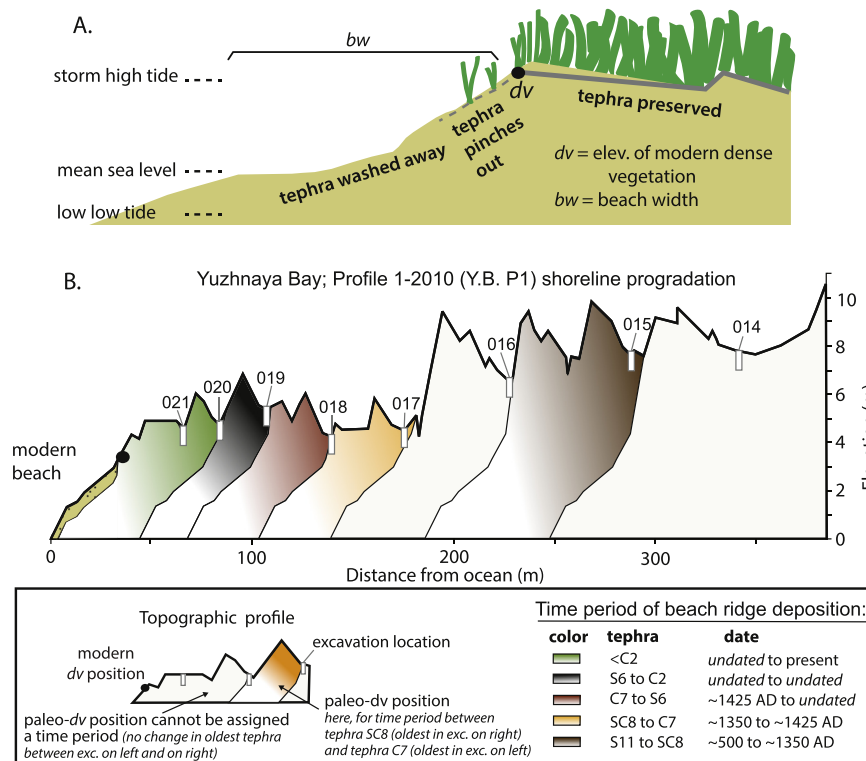


**Figure 5.** (A) Illustration of the *dv* location on the beach profile that separates where tephra can be preserved and where it is not. Modified from Pinegina et al. (2013). (B) Example illustration of the shoreline reconstruction described in the text. Note that (A) is plotted on a different scale than (B). Tephra preservation ends (paleo-*dv*) between the seaward-most excavation with the tephra and the landward-most excavation without the tephra. This method is a minimum estimate because it cannot account for possible periods of erosion that could artificially move paleo-*dv* points landward. For all reconstructions and numerical values of the calculations used in this paper, see Supplementary Figures 13–15 and Supplementary Tables 9–10.

### Paleotsunami size compared to 2006/2007

We conducted paleoshoreline analysis for all profiles in Yuzhnaya and Dushnaya bays (Fig. 5, Supplementary Figs. 13–15) and calculated or estimated paleotsunami inundation compared to the 2006/2007 deposit for all profiles (Fig. 6, Supplementary Tables 9–10). The inundation of the 2006/2007 deposit appears to be roughly typical for paleotsunami deposits in the central Kurils, with both larger and smaller paleotsunamis.

Seven paleotsunamis were larger than the 2006/2007 deposit evident on profiles YBP1 and YBP2 in Yuzhnaya Bay (recurrence average  $\sim 215 \pm 10$  yr), whereas no event was larger in the center of the bay (profile YBP216) (Supplementary Table 9). Two events since  $\sim$ AD 500 (tephra S11) are evident on profiles YBP1 and YBP2 and extend beyond the most landward excavations (recurrence average  $\sim 750 \pm 50$  yr).

Reconstructions of Dushnaya Bay give similar recurrence results as the unreconstructed analysis, but with more detail. Four paleotsunamis since the FC tephra on profile DBP2 are currently at least 11 m higher than the 2006/2007 runup on a surface above the modern coastal plain, indicating these events occur every  $310 \pm 15$  yr on average. One of these events, between the P and CC tephra, inundated at least 245–285 m inland compared to 225 m for the 2006/2007 event (Supplementary Table 10). Three events on profiles DBP12 and DBP4 had greater inundation than the 2006/2007 deposit, but only by a few 10s of meters (Fig. 6; Supplementary Table 10). On profile DBP2 the deposits from these tsunamis stop 30–100 m farther seaward than 2006/2007.

## Discussion

### Bathymetric and tsunami-source effects

Tsunamis in Ainu Bay were clearly larger than in neighboring Yuzhnaya Bay, an observation also made by the post-2006/2007 tsunami survey team (MacInnes et al., 2009a). Ainu Bay experienced severe erosion, runup of 13–20 m and inundation up to  $\sim 500$  m, while Yuzhnaya Bay experienced superficial erosion, runup of 5–8 m, and inundation of only 250 m (MacInnes et al., 2009a,b).

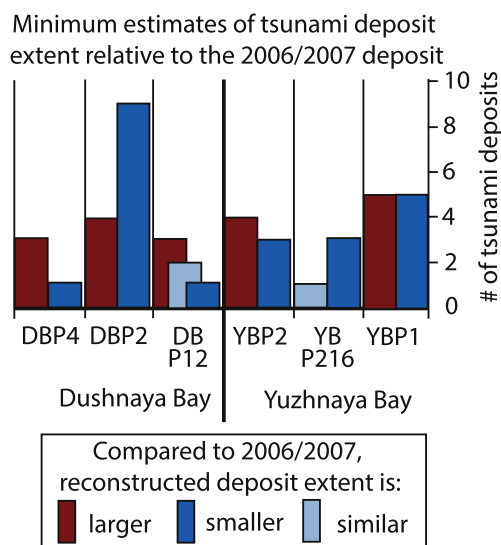


**Figure 6.** Number of tsunami deposits that are larger, smaller, or similar to the 2006/2007 tsunami deposit extent for two sites, Dushnaya Bay and Yuzhnaya Bay. Estimates could not be made for Ainu Bay both because 2006/2007 deposit extended past all excavations and because the shoreline is not a simple prograding beach ridge sequence and therefore cannot be reconstructed using our method.

Our interpretation of this recurring pattern is that the geometry of Ainu Bay naturally amplifies long wavelength waves; therefore all tsunamis will be larger in Ainu Bay compared to Yuzhnaya Bay. However, even with the amplification, the records between the two bays are similar, thus tsunamis too small to have left a record in Yuzhnaya Bay did not amplify enough in Ainu Bay to leave a sedimentary/geomorphic record. Presumably this is because the back beach height of Yuzhnaya Bay rises to just over 4 m, while the back beach (before the 2006/2007 tsunami) of Ainu Bay was around 7 m. Therefore, the topography ultimately filters what tsunamis leave a record to be similar between the two sites.

Our reconstructions of inundation show there is an anti-correlation between the inundation pattern of the 2006/2007 deposits and paleotsunami deposits: no paleotsunamis were larger than the 2006/2007 deposit on the central Yuzhnaya profile, and paleotsunamis that were slightly larger than those of 2006/2007 stopped short on the central profile in Dushnaya Bay. We suspect this difference reflects aspects of tsunami wave dynamics, where, for example, variations in wave approach angle or variations in shoaling, may explain differences between those tsunamis and the tsunami that left the 2006/2007 deposit. The 2007 aftershock of the 2006 megathrust earthquake produced a tsunami that is thought to be higher than 2006 in Yuzhnaya Bay, and may have been larger in parts of Dushnaya Bay as well (MacInnes, 2010). By normalizing all paleotsunamis to the combined 2006/2007 deposit, we may unintentionally be using an irregular deposit runup pattern reflective of an outer-rise-style event rather than a typical subduction-zone event.

### Biases that affect site fidelity and interpretation

We do not expect that we counted every tsunami that hit the central Kuril Islands because of both preservational and observational biases. These biases include location, composition and number of excavations, deposit preservation, and non-tsunami agents of sand deposition. There are differences in these potential biases amongst our study localities.

The position relative to the shoreline and the composition of excavations with good tsunami records are different for Simushir and Matua (Fig. 2). There are more excavations in peat (9 of 21 vs. 2 of 37 on Matua) in Dushnaya Bay, and those excavations are closer to the shoreline on average ( $\sim 100$  m vs.  $\sim 200$  m on Matua). Tsunami sands in peat are better preserved, whereas deposits in sandy soil are not easily distinguished from background material; thus the Dushnaya Bay record is more complete (it records more tsunamis), and this difference makes comparison with the Matua record a challenge. Our “stingy count” in peats still gave higher tsunami recurrences in Dushnaya Bay (Fig. 4D). Analysis excluding proximal coastal peats away from profiles (the profile-only count) in Dushnaya Bay yields an average tsunami recurrence ( $\sim 200$  yr) longer than on Matua ( $\sim 145$ – $160$  yr; Fig. 4E, Table 3). However, in the most recent  $\sim 600$  yr, the recurrence intervals are somewhat similar:  $\sim 45$  yr on Simushir compared to  $\sim 55$ – $75$  yr on Matua (Table 3).

Preservation bias results in a tendency for younger stratigraphy to be better preserved and over-represented compared to older stratigraphy. Fewer records remain from older time periods than from more recent ones because destructive processes, such as weathering, bioturbation and erosion remove older stratigraphy or disrupt stratigraphic coherence (e.g. Wiberg, 2000). Thus the frequency of events preserved in the geological record is typically a curvilinear function when plotted against time (Sadler, 1981; Schumer et al., 2011). For events based on stratigraphy, such as tsunami deposits, preservational bias may explain higher apparent rates for younger sediments (e.g., Pinegina et al., 2003).

The stratigraphic record will also be biased toward larger events (e.g. Wiberg, 2000), such as tsunamis that leave thicker, more

continuous, more extensive deposits. Therefore, our estimates of paleotsunami frequency potentially only reflect these larger events. Thin paleotsunami deposits from smaller events can be poorly preserved due to erosion, bioturbation, or other types of disturbances including subsequent tsunamis.

Finally, variations in climatic conditions during deposit creation and before burial, and preservation can also bias the record. In particular for the Kurils, tsunamis can transport sediment farther inland when the ground is covered in winter snow than summer grasses because the friction is lower (Minoura et al., 1996) and entrained sea ice can cause greater erosion of sediment (Razjigaeva et al., 2012). On the other hand, conditions cold enough to freeze the beach reduce the amount of sand available for transport and thus reduce the sediment inundation extent (Romundset and Bondevik, 2011). After deposition occurs, strong winds or rains can alter the deposit (e.g. Goto et al., 2011; Szczucinski, 2012), including making the deposit more or less extensive.

We found more frequent deposits in recent time intervals (Fig. 4) on both Matua and Simushir, suggesting preservational bias. Tsunami recurrence intervals calculated between present and ~AD 1400 are on the order of 45–75 yr, while those calculated between ~AD 1400 and the oldest tephra are around 75–310 yr. Because of the biases discussed above, we can conclude that the increase in the number of tsunami deposits present in younger deposits is at least partly a reflection of preservation bias. The implication, i.e., the poorer preservation of older records, implies that the more recent intervals are more representative of realistic tsunami hazards.

Another possible bias on the tsunami deposit record is the presence of sand deposits from non-tsunami sources. Beach sand can be transported inland from storm surge, storm waves or strong winds. Such sands in our study, if identified as tsunami deposits, would result in shorter estimated tsunami recurrence intervals than reality. However, storm and aeolian sand deposits can be identified as more irregular in thickness than tsunami deposits, and the zones that they affect produce overall sandy accumulations, which we avoid (Morton et al., 2007; Pinegina et al., 2013).

Our excavations were all higher than storm surge and farther inland than storm-wave washover can be reasonably expected to reach. Using the Matua tide gauge record of 1960–1982, Shevchenko and Ivinskaya (2015) analyzed the central Kurils storm record and calculated that in a 200-yr period, the likely maximum storm surge, with natural variations in tide heights, was 2.2 m, whereas our lowest excavations were at 4 m. Large storm waves added to extreme storm surges can achieve the elevation of some of our excavations, but the wavelength of storm waves does not allow significant inland penetration on high relief beach ridge plains (Morton et al., 2007). We do not use excavations in these locations because the seaward-most beach ridge has very poor soil development, thus event sands of any kind are difficult to distinguish. For similar reasons, we excavate in low areas between beach ridges, where the stratigraphy per time interval is thicker.

With regard to aeolian transport, our best estimates of the zone of possible aeolian transport, based on the density of vegetation and surficial sandiness of the soil, is ~150 m inland for Ainu Bay, and ~100 m inland for Yuzhnaya and Dushnaya bays. In the Kurils, maximum wind speeds and wind direction occur during and are controlled by cyclone storm tracks (Shevchenko and Saveliev, 1999). Wind directions would only be favorable for moving sand onto the coastal plain in cases where the southwestern quadrant of the storm passes over Dushnaya or Yuzhnaya bays and the northwest quadrant for Ainu Bay. While almost all of the excavations with good tsunami-deposit preservation used in this study are farther inland than 100–150 m, (Supplementary Figs. 5–12), a few peat excavations in Dushnaya Bay (e.g., excavations 106 and 110) (Fig. 2) lie between 60

and 100 m inland. Therefore, it is possible that aeolian deposits could affect calculated recurrence intervals for the Dushnaya-all and Dushnaya-stingy analyses; those peat excavations are not present in the Dushnaya-profile only analysis (Table 3).

#### Possible tsunami sources

Not all tsunami deposits are necessarily from directly adjacent (near-field) subduction-zone earthquakes. In the Kurils and other volcanic arcs, tsunamis can have local sources such as pyroclastic flows and volcanic sector collapses, other submarine landslides, or they can be from far-field earthquakes, either trans-oceanic or from adjacent segments of the subduction zone.

Based on the historical and geologic record of volcanoes from both sites, volcanogenic tsunamis would be more likely on Matua than Simushir. Tsunamis generated by volcanic collapses, landslides and pyroclastic flows initiate as point sources (rather than fault-line sources) and therefore dissipate over shorter distances than earthquake-generated tsunamis (Okal and Synolakis, 2004), so tsunami deposits from such events are likely only preserved on proximal islands.

The Matua record likely contains volcanogenic tsunamis, especially during Sarychev Peak's period of recent activity. For example, a 1946 eruption of Sarychev Peak on Matua (Supplementary Table 1) is documented as producing a tsunami (Soloviev and Ferchev, 1961), albeit of unknown size. Debris avalanches and pyroclastic flows have been common throughout the most recent phase of volcanism of Sarychev Peak on Matua (Gorshkov, 1958, 1967), and because Matua is small, pyroclastic flows can easily reach the sea and generate local tsunamis. Two deposits in the 20th century on Matua, between the C1a and C1b tephra (Table 2), may be from volcanic tsunamis because the correlative time period has no historical earthquakes generated in the central Kurils. Trans-Pacific tsunamis, such as from 1960 Chile, are unlikely but cannot be completely ruled out as possible sources for those deposits (see next section). Two tsunami deposits are closely associated with a cluster of cindery tephra around AD 1700–1800 (Supplementary Figs. 5–9) and were tentatively described/interpreted in the field as from volcanogenic tsunamis. Other proximal volcanoes are possible contributors to the tsunami record; for example, the nearest volcano to Matua, the tiny island of Raikoke, experienced an eruption in 1924 that was recorded to “change the outline of the island” (Gorshkov, 1967).

We expect the record in Dushnaya Bay on Simushir to contain fewer volcanogenic tsunami deposits than on Matua. While the history of volcanism near Dushnaya Bay is not as well studied as on Matua, and there are more proximal volcanoes (Fig. 2), the stratigraphy of Dushnaya Bay indicates few large eruptions, with only four local tephra in the last 2350 yr compared to 16 in the last 3300 yr for Matua (Table 2). From our analysis of Dushnaya Bay excavations, only the sand layer in the middle of the P tephra (Supplementary Figs. 10–12) is interpreted as possibly from a volcanogenic tsunami.

Other local sources of tsunami include aftershocks of megathrust earthquakes and tsunamigenic landslides. Large aftershocks of subduction zone earthquakes are known to generate local tsunamis with high runup, but these events typically closely follow subduction zone earthquakes and in such cases are unlikely to be differentiable from the main shock in the stratigraphic record. The large aftershocks in 1918, 1963, and 2007 provide good examples. Aftershocks can also trigger submarine landslides or splay faults and even generate larger tsunami runup than the preceding event, such as occurred in 1963 in the southern Kuril Islands. Razzhigaeva et al. (2008) noted that of the numerous historical tsunamis in the southern Kurils—7 in the last 50 yr—they could only distinguish

deposits from tsunamis separated by an interval of at least 20 yr. Therefore, deposits from paleotsunamis closely spaced in time would appear as one event in the geologic record. Mapping such an amalgamated deposit might result in an overestimate of the size of a tsunami from the megathrust alone, but the record would still show that a subduction zone earthquake occurred.

Not all earthquake-generated tsunamis are local; they can include tsunamis from adjacent trench segments and also trans-oceanic tsunamis. In the case of adjacent tsunamis, the southern Kurils historically have been more active than the northern Kurils, including some suggested ruptures that extended north of the Bussol Strait (see Background section). Being near the southern boundary of the central Kuril segment, Dushnaya Bay may record more tsunamis from the southern Kuril segment than Matua does from the north.

Based on the historical record, trans-Pacific tsunamis are unlikely to leave a record in our excavations. The largest trans-Pacific tsunami in the Kurils, the  $M_w$  9.5 1960 Chile event, is recorded as having 2.5 m runup on Matua Island and 3 m in Simushir Island, although the positions of these measurements are unknown (Sakhalin tsunami database <http://www.sakhgu.ru/expert/Tsunami/Tsunami.html>). A wave of only 2.5–3 m would not have left a deposit on the 4–12 m high coastal plains of Matua and Simushir. Although the historical record is short, the directionality of the 1960 Chile wave propagation suggests it is a near-maximum case for the northwest Pacific.

#### *Comparison of central Kuril sites to other segments of the JKK subduction zone*

To support the hypothesis that the JKK subduction zone is divided into southern, central, and northern segments, we might expect Matua and Simushir to exhibit paleotsunami frequencies similar to each other. If the record we produced were unexamined for biases, this hypothesis would be rejected as recurrence intervals for the two different islands are quite different, with nearly twice as many deposits in the record on Simushir than on Matua. This includes recurrence intervals of  $145 \pm 15$  yr in Yuzhnaya Bay and  $160 \pm 15$  yr in Ainu Bay on Matua, but  $65 \pm 5$  yr for all Dushnaya Bay excavations on Simushir (Table 3; Fig. 4). However, by accounting for bias associated with excavation substrate (the stingy count method) or excavation location (the profile-only method), we calculate recurrence intervals that are more similar to Matua,  $105 \pm 5$  yr or  $205 \pm 30$  yr on Simushir (Table 3), and could support the segment hypothesis.

There are reasons the Simushir intervals could be shorter than Matua, including the fact that Dushnaya Bay's key sections are closer to the ocean. Additionally, the southern Kurils had nine earthquakes  $>M_w$  7.5 in the last century and are historically more seismically active than the northern Kurils, which only experienced two earthquakes of this magnitude. Even if many southern Kuril earthquakes produced small or negligible tsunamis, only a few need leave a record on Simushir and not Matua for the recurrence interval to be shorter on Simushir.

Comparison of the central Kuril record to neighboring segments of the subduction zone show similar recurrences, but not similar patterns through time. On Matua the recurrence of deposits in the most recent 600 yr is similar to southern Kamchatka and the northern Kurils, 70–100 and ~90 yr, respectively (Pinegina, 2014). The average Simushir recurrence interval for all Dushnaya excavations is close to the 75 yr calculated for Shikotan in the southern Kurils during the time of increased seismicity there 1500 to 500 yr ago (Razzhigaeva et al., 2008). The stingy and profile-only averages are also well within the range of recurrences found in the southern Kurils record of 75–250 yr between events

(Razzhigaeva et al., 2008). Records from southern Kamchatka and the southern Kurils show an increase in seismicity from 1000 to 700 yr ago and 1500 to 500 yr ago, respectively, but a similar increase in the central Kurils at either of those times is not apparent.

The post ~AD 1400 recurrence interval of deposits on both Matua and Simushir suggests a greater frequency (potentially greater tsunami hazard) than the geologic record on most other subduction zones. Only southern Kamchatka, with recurrences as short as ~40 yr from AD 1000 to 1300 is comparable (Pinegina, 2014). On Simushir, recurrence intervals in the last 600 yr are  $45 \pm 5$  (all),  $70 \pm 5$  (stingy) and  $65 \pm 10$  (profile-only), while on Matua, the same time period had recurrence intervals of  $75 \pm 10$  yr (Yuzhnaya Bay) and  $55 \pm 5$  yr (Ainu Bay). While the last 600 yr might show a frequency above longer-term averages, we do not have a means of separating preservation bias from a real increase in frequency during this period. As discussed earlier, an increase in volcanic activity on Matua could account for shorter intervals on Matua, but cannot explain the record on Simushir, making seismicity a more likely cause if the increase is real.

The recurrence of the largest tsunamis in the central Kurils generally agrees with other segments of the JKK subduction zone, however, we note that what defines the “largest” tsunamis between sites is strongly affected by local geomorphology and such comparisons should be taken cautiously. The southern Kurils and Hokkaido indicate every 350–500 yr for the largest tsunamis, defined as  $>5$ – $7$  m elevation and  $>2.5$  km inland on Kunashir and Iturup (Iliev et al., 2005 and; Ganzey et al., 2011), and at least 1.5–2.0 km inland on Hokkaido (Sawai et al., 2009). These values are roughly similar to Simushir, where we calculated recurrence intervals of  $310 \pm 15$  yr for the largest tsunamis (defined above) using shoreline reconstructions (Table 3). In Yuzhnaya Bay on Matua, calculations show tsunamis with slightly farther inundation than 2006/2007 deposit occurred every  $215 \pm 15$  yr and largest tsunamis (defined above) every  $750 \pm 50$  yr. In general, these numbers fit in well with large and very large tsunamis in the northern Kurils and southern Kamchatka, defined as deposits comparable to 1952 Kamchatka, with runup  $>10$  m (locally  $>20$  m) and often coseismic land-level change, every 215–1100 yr and ~470 yr on average (Pinegina, 2014).

#### **Conclusion**

Paleotsunami records from the sites with the best preservation in the central Kuril Islands—Yuzhnaya Bay and Ainu Bay on Matua Island and Dushnaya Bay on Simushir Island—yield evidence of repeated tsunami inundation. The recurrence rates of these events, unfiltered for biases affecting record fidelity, are  $140 \pm 15$  yr at Yuzhnaya Bay,  $160 \pm 15$  yr at Ainu Bay, and  $65 \pm 5$  yr at Dushnaya Bay. These recurrence intervals are high, but are comparable to other segments of the Japan-Kuril-Kamchatka (JKK) subduction zone. Results from all three study areas reveal increasing number of tsunamis toward the present, which is likely due at least in part to preservation bias.

We expect that the recurrence intervals we present in Figure 4 and Table 3 are shorter than the interval of tsunamis produced by near-field subduction-zone earthquakes on the central Kuril segment because of other tsunami sources. Almost certainly, the Matua record includes volcanogenic tsunamis and the Simushir record includes tsunamis from the southern Kuril segment. We predict that the seismic cycle of large megathrust earthquakes in the central Kurils is longer than younger (post ~AD 1400) records of Matua and Simushir, but because of preservation bias, shorter than pre ~AD 1400 records.

Some paleotsunamis in the central Kurils were clearly larger than 2006/2007 tsunamis. Tsunamis at least 11 m higher than 2006/2007 deposit occurred on the order of every 300 yr on

Simushir. On Matua tsunamis that penetrated farther inland in some part of Yuzhnaya Bay occurred roughly every ~215 yr, and ones that extended at least 100 m farther inland in most of the bay occurred every ~750 yr. Although paleotsunami size is difficult to reconstruct in Ainu Bay, the record of paleotsunami frequency is comparable to Yuzhnaya Bay, and the differences in tsunami size from the 2006/2007 tsunami deposit repeats in the paleotsunami records for Yuzhnaya Bay (smaller) and Ainu Bay (larger).

Understanding the recurrence intervals of large megathrust earthquakes on the JKK subduction zone is imperative for calculating probabilistic tsunami hazard for major population and economic centers around the Pacific Rim. The relatively small 2006 and 2007 earthquakes ( $M_w$  8.3 and 8.1) demonstrated the trans-Pacific directionality of central Kuril tsunami energy towards Hawaii, California and Chile, illustrating the need to elucidate the hazard produced by this understudied region. The recurrence interval of large earthquakes on the JKK subduction zone that produce damaging, potentially trans-Pacific tsunamis is on the order of ~100 yr or higher over the last 3000 yr. Relative to many other subduction zones, such as Cascadia, Japan, and Alaska-Aleutians, this recurrence interval is shorter and therefore of importance to communities around the Pacific. In combination with the archaeological evidence for fluctuations in human settlement intensity of the Kurils (Fitzhugh, 2012; Fitzhugh et al., 2016), the results reported here provide a foundation for better human vulnerability and resilience to tsunami hazards at century to millennial time scales.

## Acknowledgments

Our co-author and dear friend Katya Kravchunovskaya died in 2013 during a mountaineering rescue on Avachinsky volcano; we miss her terribly. This research was supported by the U.S. National Science Foundation (ARC-0508109; Ben Fitzhugh, PI). The UW Center for Study of Demography and Ecology provided project support with funding from a Eunice Kennedy Shriver National Institute of Child Health and Human Development research infrastructure grant, R24 HD042828. Significant logistical support came from the Far East Branch of the Russian Academy of Sciences, Institute of Marine Geology and Geophysics, Yuzhno-Sakhalinsk, Russia (Director Boris Levin). Additional support was provided by the University of Washington (Seattle, USA); the Hokkaido University Museum (Sapporo, Japan); the Historical Museum of Hokkaido (Sapporo, Japan); the Sakhalin Regional Museum (Yuzhno-Sakhalinsk, Russia), and the Far East Branch of the Russian Academy of Sciences (IVS: Petropavlovsk-Kamchatskiy, grant RFFR-06-05-64025a (to Pinegina), NEISRI: Magadan, TIG: Vladivostok). M. Nakagawa, Hokkaido University analyzed the glass components of tephra.

## Appendix A. Supplementary data

Supplementary data related to this article can be found at <http://dx.doi.org/10.1016/j.yqres.2016.03.005>.

## References

- Ammon, C.J., Kanamori, H., Lay, T., 2008. A great earthquake doublet and seismic stress transfer cycle in the central Kuril islands. *Nature* 451, 561–566.
- Apel, E.V., Bürgmann, R., Steblow, G., Vailenko, N., King, R., Prytkov, A., 2006. Independent active microplate tectonics of northeast Asia from GPS velocities and block modeling. *Geophysical Research Letters* 33, L11303. <http://dx.doi.org/10.1029/2006GL026077>.
- Beck, S.L., Ruff, L.J., 1987. Rupture process of the great 1963 Kurile Islands earthquake sequence: asperity interaction and multiple event rupture. *Journal of Geophysical Research* 92, 14,123–14,138. <http://dx.doi.org/10.1029/JB092iB13p14123>.
- Bird, P., 2003. An updated digital model of plate boundaries. *Geochemistry, Geophysics, Geosystems* 4 (3). <http://dx.doi.org/10.1029/2001GC000252>.

- Bourgeois, J., Pinegina, T.K., Ponomareva, V.V., Zaretskaia, N.E., 2006. Holocene tsunamis in the southwestern Bering Sea, Russian Far East, and their tectonic implications. *Geological Society of America Bulletin* 118, 449–463. <http://dx.doi.org/10.1130/B25726.1>.
- Bronk Ramsey, C., 2009. Bayesian analysis of radiocarbon dates. *Radiocarbon* 51 (1), 337–360.
- Clague, J.J., Bobrowsky, P.T., Hutchinson, I., 2000. A review of geological records of large tsunamis at Vancouver Island, British Columbia, and implications for hazard. *Quaternary Science Reviews* 19 (9), 849–863.
- Dengler, L., Uslu, B., Barberopoulou, A., Yim, S.C., Kelly, A., 2009. The November 15, 2006 Kuril Islands-generated tsunami in Crescent City, California. *Pure and Applied Geophysics* 166, 37–53.
- Dura, T., Cisternas, M., Horton, B.P., Ely, L.L., Nelson, A.R., Wesson, R.L., Pilarczyk, J.E., 2015. Coastal evidence for Holocene subduction-zone earthquakes and tsunamis in central Chile. *Quaternary Science Reviews* 113, 93–111.
- Ely, L.L., Cisternas, M., Wesson, R.L., Dura, T., 2014. Five centuries of tsunamis and land-level changes in the overlapping rupture area of the 1960 and 2010 Chilean earthquakes. *Geology* 42 (11), 995–998.
- Fedotov, S.A., 1965. Regularities of the distribution of large earthquakes of Kamchatka, the Kuril Islands and north-eastern Japan. *Akademi Nauk SSSR Institute Fiziki Zemli Trudy* 36 (203), 66–93 (in Russian).
- Fedotov, S.A., 1968. On the seismic cycle, possibilities of quantitative seismic zonation, and long-term earthquake prediction. In: *Seismicheskoe raionirovanie SSSR (Seismic Zonation of the USSR)*. Nauka, Moscow, pp. 121–150.
- Fedotov, S.A., Chernyshev, S.D., Chernysheva, G.V., 1982. The improved determination of the source boundaries for earthquakes of  $M > 7.75$ , of the properties of the seismic cycle, and of long-term seismic prediction for the Kurile-Kamchatka Arc. *Earthquake Prediction Research* 1, 153–171.
- Fitzhugh, B., Shubin, V.O., Tezuka, K., Ishizuka, Y., Mandryk, C.A., 2002. Archaeology in the Kuril Islands: advances in the study of human paleobiogeography and Northwest Pacific prehistory. *Arctic Anthropology* 69–94.
- Fitzhugh, B., 2012. Chapter 1. Hazards, impacts, and resilience among hunter-gatherers of the Kuril Islands. In: Cooper, J., Sheets, P. (Eds.), *Surviving Sudden Environmental Change: Answers from Archaeology*. U. Colorado Press, Boulder, CO, pp. 19–42.
- Fitzhugh, B., Gjesfjeld, E., Brown, W., Hudson, M.J., Shaw, J.D., 2016. Resilience and the population history of the Kuril Islands, Northwest Pacific: a study in complex human ecodynamics. *Quaternary International*. <http://dx.doi.org/10.1016/j.quaint.2016.02.003>.
- Ganzev, L.A., Razjigaeva, N.G., Grebennikova, T.A., Lyashevskaya, M.S., Il'ev, A.Y., Kaistrenko, V.M., Kharlamov, A.A., 2011. Influence of natural catastrophes on the development of Southern Kuril Island landscapes in the Holocene. *Quaternary International* 237 (1), 15–23.
- Geller, R.J., Kanamori, H., 1977. Magnitudes of great shallow earthquakes from 1904 to 1952. *Bulletin of the Seismological Society of America* 67, 587–598.
- Golder, F., 1914. Russian Expansion on the Pacific, 1641–1850: an Account of the Earliest and Later Expeditions Made by the Russians along the Pacific Coast of Asia and North America; Including Some Related Expeditions to the Arctic Regions. The Arthur H. Clark co.
- Gorshkov, G.S., 1958. Catalog of the Active Volcanoes of the World Including Solfataria Fields. P. VII. Kurile Islands. *Inter. Volcanological Assoc, Napoli, Italy*, p. 99.
- Gorshkov, G.S., 1967. Volcanism of Kurile Island Arc. M.: Nauka, 287 p. (in Russian).
- Goto, K., Chagué-Goff, C., Fujino, S., Goff, J., Jaffe, B., Nishimura, Y., Richmond, B., Sugawara, D., Szczuciński, W., Tappin, D., Witter, R.C., Yulianto, E., 2011. New insights of tsunami hazard from the 2011 Tohoku-oki event. *Marine Geology* 290, 46–50. <http://dx.doi.org/10.1016/j.margeo.2011.10.004>.
- Hatori, T., 1971. Tsunami sources in Hokkaido and southern Kurile regions. *Bulletin of the Earthquake Research Institute* 49, 63–75.
- Ide, S., Baltay, A., Beroza, G.C., 2011. Shallow dynamic overshoot and energetic deep rupture in the 2011 Mw 9.0 Tohoku-Oki earthquake. *Science* 332 (6036), 1422–1429. <http://dx.doi.org/10.1126/science.1207020>.
- Iliev, A.Y., Kaistrenko, V.M., Gretskaia, E.V., Tikhonchuk, E.A., Razjigaeva, N.G., Grebennikova, T.A., Ganzev, L.A., Kharlamov, A.A., 2005. Holocene tsunami traces on Kunashir Island, Kurile subduction zone. In: Satake, K. (Ed.), *Tsunamis: Case Studies and Recent Developments; Advances in Natural and Technological Hazards Research*. Springer, Netherlands, pp. 171–192.
- Kelsey, H.M., Nelson, A.R., Hemphill-Haley, E., Witter, R.C., 2005. Tsunami history of an Oregon coastal lake reveals a 4650 yr record of great earthquakes on the Cascadia subduction zone. *Geological Society of America Bulletin* 117, 7–8, 1009–1032.
- Krashennnikov, S.P., 1972. Explorations of Kamchatka, North Pacific Scimitar; Report of a Journey Made to Explore Eastern Siberia in 1735–1741, by Order of the Russian Imperial Government. Oregon Historical Society, Portland.
- Laverov, N.P., Dobrezov, N.L., Bogatikov, O.A., Bondur, V.G., Gurbaniv, A.G., Karamurzov, B.S., Kovalenko, V.I., 2005. Modern and Holocene Volcanism in Russia. Nauka, Moscow, 604 pp. [in Russian].
- Laverov, N.P., Lappo, S.S., Lobkovsky, L.L., Baranov, B.V., Kulnich, R.G., Karp, B.Y., 2006. The central Kuril “gap”: structure and seismic potential. *Doklady Earth Science* 409, 787–790. <http://dx.doi.org/10.1134/S1028334X06050254>.
- Lay, T., Kanamori, H., Ammon, C.J., Hutko, A.R., Furlong, K., Rivera, L., 2009. The 2006–2007 Kuril Islands great earthquake sequence. *Journal of Geophysical Research* 114, B11308. <http://dx.doi.org/10.1029/2008JB006280>.
- Lensen, G.A., 1959. *The Russian Push toward Japan; Russo-Japanese Relations, 1697–1875*. Princeton University Press, Princeton, NJ.

- MacInnes, B.T., 2010. Bridging Seismology and Geomorphology: Investigations of the 2006 and 2007 Kuril Island Tsunamis. Ph.D. dissertation. University of Washington, Seattle, 177 pp.
- MacInnes, B.T., Weiss, R., Bourgeois, J., Pinegina, T.K., 2010. Slip distribution of the 1952 Kamchatka great earthquake based on near-field tsunami deposits and historical records. *Bulletin of the Seismological Society of America*. <http://dx.doi.org/10.1785/0120090376>.
- MacInnes, B.T., Pinegina, T.K., Bourgeois, J., Razhegava, N.G., Kaistrenko, V.M., Kravchunovskaya, E.A., 2009a. Field survey and geological effects of the 15 November 2006 Kuril tsunami in the middle Kuril Islands. *Pure and Applied Geophysics* 166. <http://dx.doi.org/10.1007/s00024-008-0428-3>.
- MacInnes, B.T., Bourgeois, J., Pinegina, T.K., Kravchunovskaya, E., 2009b. Tsunami geomorphology: erosion and deposition from the 15 November 2006 Kuril Island tsunami. *Geology* 37, 995–998.
- MacInnes, B., Fitzhugh, B., Holman, D., 2014. Controlling for landform age when determining the settlement history of the Kuril Islands. *Geoarchaeology* 29 (3), 185–201.
- Mackey, K.G., Fujita, K., Gunbina, L., Kovalev, V., Imaev, V., Kozmin, B., 1997. Seismicity of the Bering Strait region: evidence for a Bering block. *Geology* 25, 979–982. [http://dx.doi.org/10.1130/0091-7613\(1997\)025<0979:SOTBSR>2.3.CO;2](http://dx.doi.org/10.1130/0091-7613(1997)025<0979:SOTBSR>2.3.CO;2).
- Minoura, K., Gusiakov, V.G., Kurbatov, A., Takeuti, S., Svendsen, J.I., Bondevik, S., Oda, T., 1996. Tsunami sedimentation associated with the 1923 Kamchatka earthquake. *Sedimentary Geology* 106 (1), 145–154.
- Miyatake, K., 1934. On the explosion of volcano Harumukotan-jima, central Kurile (Chishima), in Jan., 1933. *Bulletin of the Volcanological Society of Japan* 2, 76–85 (in Japanese).
- Morton, R.A., Gelfenbaum, G., Jaffe, B.E., 2007. Physical criteria for distinguishing sandy tsunami and storm deposits using modern examples. *Sedimentary Geology* 200, 184–207.
- Nakagawa, M., Ishizuka, Y., Hasegawa, T., Baba, A., Kosugi, A., 2008. Preliminary Report on Volcanological Research of KBP 2007–08 Cruise by Japanese Volcanology Group. The Digital Archaeological Record, tDAR ID: 391304. <http://dx.doi.org/10.6067/XCV8668F2H>.
- Nanayama, F., Satake, K., Furukawa, R., Shimokawa, K., Atwater, B.F., Shigeno, K., Yamaki, S., 2003. Unusually large earthquakes inferred from tsunami deposits along the Kuril trench. *Nature* 424 (6949), 660–663.
- National Geophysical Data Center/World Data Service (NGDC/WDS). Global Historical Tsunami Database. National Geophysical Data Center, NOAA. doi: 10.7289/V5PN93H7 (accessed 2014).
- Nelson, A.R., Briggs, R.W., Dura, T., Engelhart, S.E., Gelfenbaum, G., Bradley, L.-A., Forman, S.L., Vane, C.H., Kelley, K.A., 2015. Tsunami recurrence in the eastern Alaska-Aleutian arc: a Holocene stratigraphic record from Chirikof Island, Alaska. *Geosphere* 11 (4). <http://dx.doi.org/10.1130/GES01108.1>.
- Nelson, A.R., Kelsey, H.M., Witter, R.C., 2006. Great earthquakes of variable magnitude at the Cascadia subduction zone. *Quaternary Research* 65 (3), 354–365.
- Ogryzko, I.I., 1953. Discovery of Kurile Islands, *The Scientific Notes of Leningrad State University, Faculty of Northern People*, vol. 2, p. 157.
- Okal, E., 1992. Use of mantle magnitude  $M_m$  for the reassessment of the moment of historical earthquakes I: shallow events. *Pure and Applied Geophysics* 139, 17–57.
- Okal, E.A., Synolakis, C.E., 2004. Source discriminants for near-field tsunamis. *Geophysical Journal International* 158 (3), 899–912.
- Pacheco, J.F., Sykes, L.R., 1992. Seismic moment catalog of large shallow earthquakes, 1900 to 1989. *Bulletin of the Seismological Society of America* 8, 1306–1349.
- Pinegina, T., 2014. Time-space Distribution of Tsunamiogenic Earthquakes along the Pacific and Bering Coasts of Kamchatka: Insight from Paleotsunami Deposits. Doctor of Geological Science dissertation. Institute of Oceanology RAS, Moscow, 235 pp. [in Russian].
- Pinegina, T.K., Bourgeois, J., Bazanova, L.I., Melekestsev, I.V., Braitseva, O.A., 2003. A millennial-scale record of Holocene tsunamis on the Kronotskiy Bay coast, Kamchatka, Russia. *Quaternary Research* 59 (1), 36–47.
- Pinegina, T.K., Bourgeois, J., Kravchunovskaya, E.A., Lander, A.V., Arcos, M.E., Pedoja, K., MacInnes, B.T., 2013. A nexus of plate interaction: vertical deformation of Holocene wave-built terraces on the Kamchatsky Peninsula (Kamchatka, Russia). *Geological Society of America Bulletin* 125, 9–10, 1554–1568.
- Rabinovich, A.B., Lobkovsky, L.I., Fine, I.V., Thomson, R.E., 2008. Source observations and modeling of the Kuril Islands tsunamis of 15 November 2006 and 13 January 2007. *Advances in Geosciences* 14, 105–116.
- Razzhigaeva, N.G., Ganzey, L.A., Grebennikova, T.A., Kharlamov, A.A., Ilyev, A.Y., Kaistrenko, V.M., 2008. The geological record of paleotsunamis striking Shikotan Island, in the lesser Kurils, during Holocene time. *Journal of Volcanology and Seismology* 2 (4), 262–277.
- Razjigaeva, N.G., Ganzey, L.A., Grebennikova, T.A., Ivanova, E.D., Kharlamov, A.A., Kaistrenko, V.M., Shishkin, A.A., 2012. Coastal sedimentation associated with the Tohoku tsunami of 11 March 2011 in South Kuril Islands, NW Pacific Ocean. *Pure and Applied Geophysics*. <http://dx.doi.org/10.1007/s00024-012-0478-4>.
- Romundset, A., Bondevik, S., 2011. Propagation of the Storegga tsunami into ice-free lakes along the southern shores of the Barents Sea. *Journal Of Quaternary Science* 26 (5), 457–462. <http://dx.doi.org/10.1002/jqs.1511>.
- Sadler, P.M., 1981. Sediment accumulation rates and the completeness of stratigraphic sections. *The Journal of Geology* 569–584.
- Sawai, Y., Kamataki, T., Shishikura, M., Nasu, H., Okamura, Y., Satake, K., Thomson, K.H., Matsumoto, D., Fujii, Y., Komatsubara, J., Aung, T.T., 2009. Aperiodic recurrence of geologically recorded tsunamis during the past 5500 years in eastern Hokkaido, Japan. *Journal of Geophysical Research: Solid Earth* (1978–2012) 114 (B1).
- Schumer, R., Jerolmack, D., McElroy, B., 2011. The stratigraphic filter and bias in measurement of geologic rates. *Geophysical Research Letters* 38 (11). <http://dx.doi.org/10.1029/2011GL047118>.
- Shevchenko, G., Ivetskaya, T., 2015. Estimation of extreme sea levels for the Russian coasts of the Kuril Islands and the Sea of Okhotsk. *Pure and Applied Geophysics*. <http://dx.doi.org/10.1007/s00024-015-1077-y>.
- Shevchenko, G., Saveliev, V.Yu., 1999. Spatial variability of the wind field in the area of the Kuril Islands. In: *Proceedings of the Second Workshop on the Okhotsk Sea and Adjacent Areas*, 12, pp. 49–53. PICES Sci. Rep.
- Soloviev, S.L., Ferchev, M.D., 1961. Summary of data on tsunamis in the USSR. *Bulletin of the Council for Seismology* 9, 1–37 (in Russian).
- Song, T.A., Simons, M., 2003. Large trench-parallel gravity variations predict seismic behavior in subduction zones. *Science* 301, 630–633. <http://dx.doi.org/10.1126/science.1085557>.
- Sugawara, D., Imamura, F., Matsumoto, H., Goto, K., Minoura, K., 2010. Numerical reconstruction of ancient tsunami: field survey of the Jogan tsunami and estimation of paleo-topography. *DCRC tsunami engineering* 27, 103–132 (in Japanese).
- Szczuciński, W., Kokociński, M., Rzeszewski, M., Chagué-Goff, C., Cachão, M., Goto, K., Sugawara, D., 2012. Sediment sources and sedimentation processes of 2011 Tohoku-oki tsunami deposits on the Sendai Plain, Japan—Insights from diatoms, nannoliths and grain size distribution. *Sedimentary Geology* 282, 40–56. <http://dx.doi.org/10.1016/j.sedgeo.2012.07.019>.
- Tanigawa, K., Sawai, Y., Shishikura, M., Namegaya, Y., Matsumoto, D., 2014. Geological evidence for an unusually large tsunami on the Pacific coast of Aomori, northern Japan. *Journal of Quaternary Science* 29 (2), 200–208.
- Wiberg, P., 2000. A perfect storm: formation and potential for preservation of storm beds on the continental shelf. *Oceanography* 13 (3), 93–99. <http://dx.doi.org/10.5670/oceanog.2000.18>.
- Witter, R.C., Kelsey, H.M., Hemphill-Haley, E., 2003. Great Cascadia earthquakes and tsunamis of the past 6700 years, Coquille River estuary, southern coastal Oregon. *Geological Society of America Bulletin* 115 (10), 1289–1306.